Ocean Modelling 23 (2008) 73–81

Contents lists available at ScienceDirect

Ocean Modelling

journal homepage: www.elsevier.com/locate/ocemod

Time splitting and linear stability of the slow part of the barotropic component

Yves Morel [a,*], Remy Baraille [a], Annick Pichon [b]

[a] SHOM (site de Meteo-France), 42 av. Gaspard Coriolis, 31057 Toulouse, France
[b] SHOM/HOM/REC, BP30316, 29603 Brest Cedex, France

ARTICLE INFO

Article history:
Received 22 December 2007
Received in revised form 21 March 2008
Accepted 1 April 2008
Available online 22 April 2008

Keywords:
Numerical schemes
Linear stability
Time splitting

ABSTRACT

In this paper, the authors analyse the stability of particular numerical schemes used in oceanic general circulation models to deal with the barotropic momentum advection term. It is shown that, when this term is integrated using time splitting, its stability properties can be drastically reduced in configurations where there exists shallow areas, where velocities become comparable to the propagation speed of external gravity waves. A simple alternative scheme with improved stability is proposed and discussed.

1. Introduction

Many primitive equation models use time splitting techniques to deal with the fast propagation of external gravity waves: there exists a set of baroclinic equations and a set of barotropic equations, respectively dealing with the so-called slow terms (often called baroclinic mode) and fast terms (barotropic mode), the latter using a time step that is much smaller than the former. Most models integrate all purely barotropic terms inside the barotropic equations. In practice, only the pressure gradient and barotropic mass flux terms are associated with the external gravity waves and all other terms could be treated during the slow evolutions step with the larger baroclinic time step, which reduces the computational cost.

This is what is done in the Miami Isopycnic Coordinate Ocean Model (MICOM) or the HYbrid Coordinate Ocean Model (HYCOM)[1] for which the barotropic velocity diffusion terms and barotropic advection terms are calculated during the baroclinic step and used as a constant forcing term during the barotropic integration (see Bleck and Boudra, 1986; Bleck and Smith, 1990; Bleck et al., 1992; Bleck, 2002).

While testing HYCOM (see Bleck, 2002) in high resolution configurations with strong tides and shallow areas, we have, however, been faced with unexpected numerical instabilities related to this numerical choice. Indeed, removing the momentum advection term or removing the barotropic component suppressed the instabilities. Reducing the barotropic time step did not suppress the problem, and sometimes even made it worse. Stability could only be recovered with very small baroclinic time steps. All these tests identified the barotropic momentum advection term as the source of the observed numerical instabilities which, we will show, can be expected with the MICOM or HYCOM original schemes when the velocity is non-negligible in comparison with the external gravity wave propagation speed, that is to say in shallow areas. For the time splitting method mentioned above, the treatment of the entire barotropic component involves both sets of baroclinic and barotropic equations and their coupling, which make the stability analysis of the barotropic component less straightforward than other models. As a matter of fact, previous publications on MICOM and HYCOM models (see Bleck and Boudra, 1986; Bleck and Smith, 1990; Bleck et al., 1992; Bleck, 2002) did not address the latter topic. Many papers deal with the problem of the time splitting and instability associated with aliasing of the fast into the slow modes which can lead to numerical instability when there remain "traces" of the fast external gravity waves in the baroclinic equations (see Higdon and Bennet, 1996; Hallberg, 1997; Shchepetkin and McWilliams, 2005), but to our knowledge no one has ever studied in detail the stability of the slow part of the barotropic component when it is calculated during the baroclinic step and combined with time splitting. This is the main topic of the present article. The paper is organised as follows: the equations and their analytical solutions are presented in the second section; the stability properties of the original HYCOM or MICOM scheme is analysed in Section 3 and some alternative schemes are then proposed and tested (fourth section). Our results are summed up and discussed in the last section, in particular, even though our work focuses on the MICOM and HYCOM models, we examine the cost effectiveness of alternative schemes, which can be useful for other models too.

* Corresponding author.
E-mail addresses: yves.morel@shom.fr (Y. Morel), baraille@cmo-tlse.shom.fr (R. Baraille), annick.pichon@shom.fr (A. Pichon).

[1] Notice the barotropic Coriolis term is also retained in the barotropic equation in these models.

1463-5003/$ - see front matter © 2008 Elsevier Ltd. All rights reserved.
doi:10.1016/j.ocemod.2008.04.001

2. Equations and analytical solutions

2.1. Equations

We consider the shallow water equations (see Cushman-Roisin, 1994; Pedlosky, 1987), in one dimension (we assume $\partial_y = 0$) and without Coriolis terms. These equations are

$$\begin{aligned} &\partial_T U + U\partial_X U = -g\partial_X Z + F_X, \\ &\partial_T H + \partial_X(HU) = 0, \end{aligned} \tag{1}$$

where U represents the horizontal component of the velocity field, Z is the sea surface elevation, H is the water column thickness, so that $Z = H - H_0$ where H_0 is the thickness at rest, and g the earth gravity. F_X is a dissipation term that will be neglected in the present study.

To analyse the linear stability of Eq. (1), we assume periodicity of the solutions and linearise the previous equations around the reference state (U_0, H_0) where U_0 and H_0 are constant parameters and represent a stationary current flowing over a flat bottom. We also non-dimensionalise the equations using ΔX for the horizontal length scale (which will be associated with the grid size when the equations will be discretised), H_0 for the vertical length scale (used to non-dimensionalise Z), and $\Delta X/\sqrt{gH_0}$ for time. The linearised equations for the non-dimensional perturbation $(u, \zeta) = ((U - U_0)/U_0, Z/H_0)$ are then (with dissipation terms neglected)

$$\begin{aligned} &\partial_t u = -u_0\partial_x u - \partial_x \zeta, \\ &\partial_t \zeta = -u_0\partial_x \zeta - \partial_x u, \end{aligned} \tag{2}$$

where $t = T\sqrt{gH_0}/\Delta X$ is the non-dimensional time, $x = X/\Delta X$ the non-dimensional horizontal coordinate and $u_0 = U_0/\sqrt{gH_0}$ the non-dimensional background velocity. Notice that u_0 is a small parameter except in very shallow coastal areas ($H_0 \leqslant 10$ m or so).

2.2. Analytical solutions

Eqs. (2) can be solved using Fourier transforms. The free solutions are

$$(u_k, \zeta_k) = \alpha_k^+(1, 1)e^{i(kx - C^+ t)} + \alpha_k^-(-1, 1)e^{i(kx - C^- t)}, \tag{3}$$

where

$$\begin{aligned} &C^+ = u_0 + 1, \\ &C^- = u_0 - 1 \end{aligned} \tag{4}$$

are the two possible propagation speeds, k is the non-dimensional wavenumber and (α_k^+, α_k^-) are parameters determining the solution and can be calculated given the initial structure of the perturbation.

Notice that the propagation speed does not depend on the wavenumber k, and the waves are thus non-dispersive, a well-known result. The solution can thus easily be expressed in the physical space as a function of the initial conditions. We have, however, kept the wavenumber formulation as the tests we have made are based on monochromatic waves instead of isolated perturbations or other shapes.

2.3. Approximate equations solved in MICOM or HYCOM

In the MICOM (see Bleck and Boudra, 1986; Bleck and Smith, 1990; Bleck et al., 1992) or HYCOM (see Bleck, 2002) models, the continuity equation is simplified and H is replaced by H_0 in the barotropic continuity equation (and $u_0\partial_x\zeta$ is neglected) so that the equations solved instead of (2) are

$$\begin{aligned} &\partial_t u = -u_0\partial_x u - \partial_x \zeta, \\ &\partial_t \zeta = -\partial_x u, \end{aligned} \tag{5}$$

whose analytical solutions are

$$(u_k, \zeta_k) = \alpha_k^+(C^+, 1)e^{i(kx - C^+ t)} + \alpha_k^-(C^-, 1)e^{i(kx - C^- t)} \tag{6}$$

with

$$\begin{aligned} C^+ &= \frac{1}{2}u_0 + \sqrt{1 + \frac{u_0^2}{4}}, \\ C^- &= \frac{1}{2}u_0 - \sqrt{1 + \frac{u_0^2}{4}}, \end{aligned} \tag{7}$$

which are different from the true solutions (3) and (4) when u_0 is not negligible. This is the case in shallow coastal areas ($H_0 \leqslant 10$ m or so). Notice, however, that there is no additional dispersion associated with the simplification (5): the waves are still non-dispersive, only their actual propagation speed changes. Finally, note that the results discussed below are not changed if Eq. (2) are used instead of (5).

3. Numerical solutions

Numerical solutions of (2) or (5) are calculated using space and time discretisation with respective non-dimensional elementary steps $\Delta x = 1$ and $\Delta t = \Delta T\sqrt{gH_0}/\Delta X$. Any function of time and space then takes the form $\Phi_j^N = \Phi(j\Delta x, N\Delta t)$. For explicit numerical schemes, the time step Δt has to be chosen carefully to avoid linear instability. The Courant–Friedrich–Levy (CFL) criterion constrains the time step, which must generally be chosen so that the Courant number $C\Delta T/\Delta X$, where C is the propagation speed of the fastest waves, is below a constant α whose value depends on the numerical scheme but is generally close to 1. Notice the non-dimensional time step Δt is the Courant number associated with external gravity wave propagation. Finally, we will consider second order centered spatial schemes, on a C grid (see Arakawa and Lamb, 1977).

3.1. Time splitting

Gravity waves are generally the fastest waves represented by the equations, and a small time step must be used to calculate their evolution. They are associated with the terms $\partial_x\zeta$ and $\partial_x u$ in Eq. (2) or (5). The advective terms $u_0\partial_x$ are generally associated with a much slower evolution, so that larger time steps can be used to calculate them numerically. Despite this property, in many numerical models these terms are solved together with the fast gravity waves, probably because of the way the codes have been constructed: generally 3-D codes are constructed on the basis of barotropic (2-D) codes which integrate all purely barotropic terms with the same short time step (limited by the fast gravity waves for explicit schemes). As it seems natural to save computational time when possible, some numerical models have however chosen to calculate advective terms with larger time steps. To do so, these terms are incorporated in the slow, or baroclinic, equations, for which the time step is generally limited by the internal gravity waves (or advective terms themselves) and is often an order of magnitude above the barotropic time step. This is the case for the MICOM and HYCOM models (see Bleck and Smith, 1990, Bleck, 2002).[2]

In practice in the HYCOM model, Eqs. (5) (or (2)) are solved in the following manner (see Fig. 1):

[2] As discussed above, in MICOM and HYCOM, the advective term is originally neglected in the continuity equation. We have, however, reintegrated this term to deal with very shallow areas but in order to preserve conservation and positivity of the water depth, the flux form of the barotropic continuity equation has to be maintained. The barotropic advective term of the continuity equation then has to be calculated with the divergence term during the barotropic step, thus using the barotropic time step.

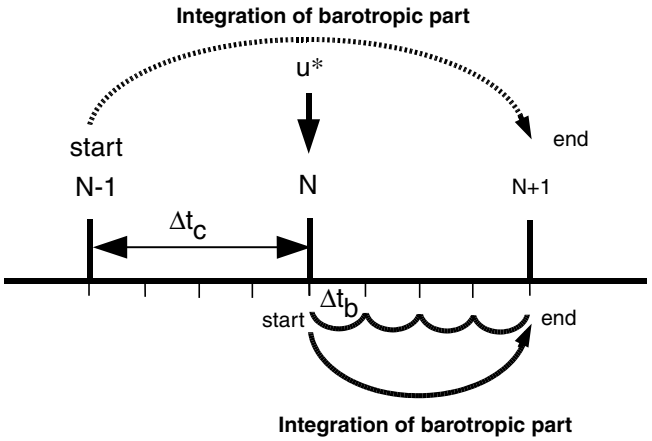

Fig. 1. Schematic of the MICOM/HYCOM time integration. The baroclinic step uses a leapfrog scheme and the u^* term is calculated at time $N\Delta t_c$. The barotropic integration starts at time step $N\Delta t_c$, so that the slow term evolution, associated with u^*, is integrated, on average, with a Euler time stepping scheme during the barotropic step.

First the slow evolution of the velocity field is calculated with a large time step Δt_c:

$$\partial_t u = -u_0 \partial_x u = u^*. \tag{8}$$

The velocity field is advanced from time $(N-1)\Delta t_c$ to time $(N+1)\Delta t_c$ using a leapfrog scheme, thus

$$u^* = -u_0(u^N_{j+1} - u^N_{j-1}). \tag{9}$$

Then the fast gravity waves are calculated from time $N\Delta t_c$ to time $(N+1)\Delta t_c$ with a smaller time step Δt_b. To do so, we need to ensure that $\Delta t_c = N_0 \Delta t_b$ where N_0 is an integer (and is even in HYCOM, for purposes related to the Coriolis term, see Bleck and Smith, 1990). During the integration of the fast waves, the momentum advection term is considered constant and comes from the slow evolution. We thus have for the fast mode:

$$\begin{aligned} \partial_t u &= -\partial_x \zeta + u^*, \\ \partial_t \zeta &= -\partial_x u(-u_0 \partial_x \zeta). \end{aligned} \tag{10}$$

At the end of the integration of the barotropic equations, the velocity and free surface fields at time $(N+1)\Delta t_c$ take into account all (slow and fast) evolution terms.

3.2. Numerical schemes for the fast mode

In this paper, we concentrate on the stability of the barotropic momentum advection term, associated with u^*. The implementation described above makes use of time splitting for this term, and the numerical scheme associated with Eq. (10) is thus important, as well as its proper stability properties. To avoid confusion, we only recall the numerical scheme used for the fast mode below, and the discussion of its properties is dismissed to Appendix A (where new schemes with improved stability are also proposed).

To numerically solve Eq. (10), different temporal schemes can be used. The Euler forward–backward scheme is mentioned as the scheme used in MICOM or HYCOM (see Bleck and Smith, 1990), but in practice, it has been mixed with the leapfrog scheme: MICOM or HYCOM indeed mix the time derivatives of both Euler forward–backward and leapfrog schemes while the spatial terms only use the Euler forward–backward form. A new coefficient is introduced to do so, $\bar{w}$ (called *wbaro* in the code). Finally, the numerical scheme used in MICOM or HYCOM for Eq. (10) is

$$\begin{aligned} \zeta^{n+1}_j &= (1-\bar{w})\zeta^n_j + \bar{w}\zeta^{n-1}_j - (1+\bar{w})\frac{\Delta t}{\Delta x}(u^n_{j+1} - u^n_j), \\ u^{n+1}_j &= (1-\bar{w})u^n_j + \bar{w}u^{n-1}_j - (1+\bar{w})\frac{\Delta t}{\Delta x}(\zeta^{n+1}_j - \zeta^{n+1}_{j-1}). \end{aligned} \tag{11}$$

Notice that when $\bar{w} = 0$, the pure Euler forward–backward scheme is recovered, whereas when $\bar{w} = 1$ we end up with a leapfrog forward–backward scheme, which is unconditionally unstable.

3.3. Stability of the slow term u^*

In MICOM or HYCOM, Eq. (11) are integrated over one baroclinic time step, from time $N\Delta t_c$ (corresponding to $n = 0$) to $(N+1)\Delta t_c$ (corresponding to $n = N_0$, see Fig. 1). As a first step to analyse the stability associated with the slow term u^*, we can consider a pure advection and neglect all fast terms from Eq. (10). As u^* is constant during the integration of Eq. (11), we end up with a Euler scheme (integration from $N\Delta t_c$ to $(N+1)\Delta t_c$) for the average time stepping scheme for u^*. Advection calculated with a Euler time stepping and a centered spatial scheme (Eq. (9)) is unconditionally unstable, and numerical instabilities can thus be expected with the MICOM/HYCOM original scheme at least when advection is non-negligible in comparison with the gravity wave terms, that is to say in shallow areas. For depth typical of oceanic basins ($H_0 \simeq 1000$ m or so), the gravity wave terms dominate which may play a stabilising role for the unstable advective terms, but this is not obvious and an analysis of the stability properties of the slow barotropic component is necessary.

3.4. Analysis method for the stability of the slow barotropic component

Because of the time splitting technique, it is not easy to evaluate the stability of the slow component, as the effect of the integration of the fast waves over a baroclinic time step has to be taken into account. The technique we propose first relies on an analysis for each spatial mode associated with a given wavenumber k. We thus rewrite the discretised equations for solutions of the form

$$\begin{aligned} u^N_j &= \hat{u}^N_k e^{ikj\Delta x}, \\ \zeta^N_j &= \hat{\zeta}^N_k e^{ikj\Delta x}. \end{aligned} \tag{12}$$

As Eqs. (2) or (5) are linear, if we hypothesize that the velocity and free surface fields at time $(N+1)\Delta t_c$ only depend on the same fields at time $N\Delta t_c$ and $(N-1)\Delta t_c$ (see Appendix B for a justification and discussion of this hypothesis), then after full integration, because of the linearity of the barotropic equations, the fields at the new time step are necessarily of the form:

$$(\hat{u}^{N+1}_k, \hat{\zeta}^{N+1}_k) = \mathbf{A}_k(\hat{u}^N_k, \hat{\zeta}^N_k) + \mathbf{B}_k(\hat{u}^{N-1}_k, \hat{\zeta}^{N-1}_k), \tag{13}$$

where $\mathbf{A}_k$ and $\mathbf{B}_k$ are 2×2 matrices which can be calculated numerically using the equations for the solutions of the form (12) (see Appendix B). The linear stability of the scheme can then be evaluated using the recurrence relation (13) and looking for solutions $(\hat{u}^N_k, \hat{\zeta}^N_k) = \lambda^N(\hat{u}_k, \hat{\zeta}_k)$ (see Appendix B).

The plain line in Fig. 2 represents the results for the stability of the original MICOM or HYCOM scheme as a function of $\Delta t_c = N_0 \Delta t_b$ and u_0, for $\bar{w} = 0.125$ and $\Delta t_b = 0.5$. For comparison, the dotted curve represents the ideal CFL stability curve for a pure advective model with a leapfrog time stepping scheme (associated with the criterion $u_0 \Delta t_c \leqslant 1$). Notice that the real curve is always far below the latter stability, and that for velocity $u_0 > 0.1$ or so, it is always unstable. However, this also shows that the presence of gravity waves have indeed a stabilising effect (remember that the scheme should be unconditionally unstable for pure advection).

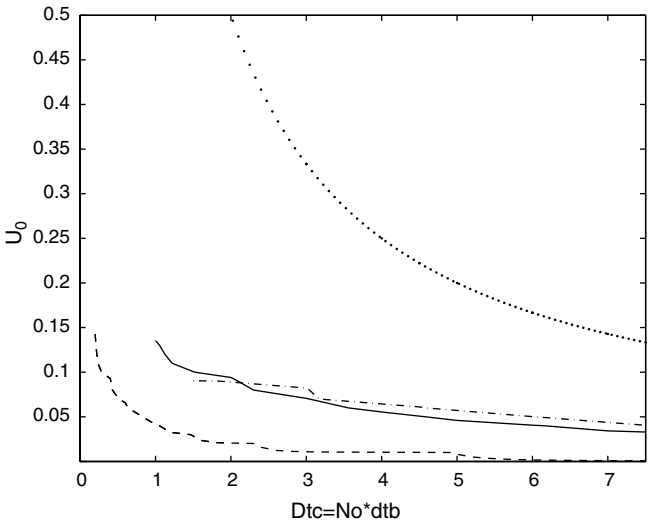

Fig. 2. Stability of the slow part of the barotropic component for the MICOM/HYCOM scheme, as a function of the slow time step Δt_c and background velocity $u_0(\bar{w} = 0.125)$. Different barotropic time steps have been tested: $\Delta t_b = 0.5$ (plain), $\Delta t_b = 0.1$ (dashed), $\Delta t_b = 0.75$ (dash–dotted). The dotted curve represents the CFL criterion for a pure advection treated with a leapfrog scheme.

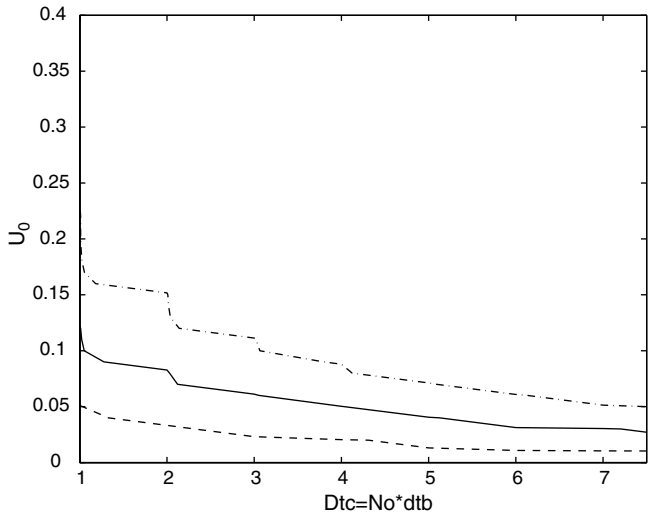

Fig. 3. Stability of the slow part of the barotropic component for the MICOM/HYCOM scheme, as a function of the slow time step Δt_c and background velocity u_0 ($\Delta t_b = 0.5$), for different choices of $\bar{w}$: $\bar{w} = 0.125$ (plain), $\bar{w} = 0.05$ (dashed), $\bar{w} = 0.25$ (dash–dotted).

3.5. Sensitivity study

Fig. 2 also represents the results for different choices of the fast time step: $\Delta t_b = 0.1$ is the dashed line and $\Delta t_b = 0.75$ the dash–dotted line. Notice that smaller fast time steps lead to less stability, the best stability being achieved for the largest Δt_b. This unexpected behaviour is a feature of the instability of the slow part of the barotropic component which can be hidden because other terms (barotropic gravity waves but also other baroclinic terms in realistic configurations) are also important and can stabilise the total scheme. u_0 is indeed usually very small: typically less than 0.01 when the minimum depth of the basin exceeds 100 m or so, but reaches 0.1 or more when the minimum depth reaches typically 10 m and with strong barotropic currents (1 m s^{-1}). It is interesting to notice that some users have experienced unexplained instabilities of the HYCOM code with some realistic configuration, and the way they found to stabilise the code was to impose a limit for the minimum depth (Geir Evensen, personal communication, 2002). This indeed ensures stability as it bounds the non-dimensional velocity u_0, which is consistent with the present results (see below too).

As the numerical schemes associated with the slow evolution of the barotropic velocity field are unstable, and seem only stabilised by implicit numerical diffusion, we test the sensitivity of this instability to different parameters, in particular associated with some diffusion.

This is the case of the parameters $\bar{w}$. Fig. 3 is the same as Fig. 2 but with different choices of the parameter $\bar{w}$ ($\Delta t_b = 0.5$ is fixed): $\bar{w} = 0.125$ the classical HYCOM value (plain line), $\bar{w} = 0.05$ (dashed line) and $\bar{w} = 0.25$ (dash–dotted line). A test with $\bar{w} = 0$ has shown that this choice, which would have allowed the highest barotropic time step for the barotropic scheme ($\Delta t_b = 1$), leads to unconditional instability as soon as $u_0 \neq 0$, which we believe explains the fact that, in practice, the pure Euler forward–backward scheme for the fast mode is impossible and that it was necessary to mix this scheme with leapfrog to ensure stability in realistic configurations (see Appendix A). Also, for $\bar{w}$ above a certain value, the fast numerical schemes become unstable (see Appendix A), which also transmits instability to the slow component. Notice that, for the chosen fast time step ($\Delta t_b = 0.5$), the maximum admissible value for $\bar{w}$ is $\bar{w} \simeq 0.33$ (see Fig. 8 in Appendix A).

To conclude this analysis of the original MICOM/HYCOM stability, we have repeated the same experiment as in Fig. 3 but with different choices of the fast time step Δt_b. We have found that the optimal value of $\bar{w}$ for stability is highly variable, from $\bar{w} = 0.125$ for $\Delta t_b = 0.75$ to $\bar{w} = 0.75$ for $\Delta t_b = 0.1$. So that the way the mixed MICOM/HYCOM scheme can stabilise the apparent instability of the slow part of the barotropic component is not obvious, and we have not found a rule for the choice of the optimal $\bar{w}$ that could be applied to realistic cases with varying bottom topography (for which the non-dimensional parameter Δt_b would vary over a wide interval). We may thus wonder if another choice for the treatment of the advective term, in particular ensuring stability, would not lead to easier choices or even better results. This is the subject of the next section.

4. Modifications of the numerical schemes

4.1. Alternative schemes

The first obvious choice to ensure stability of the slow barotropic evolution in MICOM/HYCOM is to integrate the advective term together with the fast terms. With such a choice, the barotropic advection term must be withdrawn from the baroclinic equations for each vertical level and recomputed after in the barotropic equation every barotropic time step. This solution is obviously more expensive than the original MICOM/HYCOM scheme, but it leads to a scheme that is stable over a baroclinic time step, regardless of its duration, as long as the barotropic scheme is stable itself. The scheme writes

$$\begin{aligned} &u^* = 0, \\ &\partial_t u = -\partial_x \zeta - u_0 \partial_x u, \\ &\partial_t \zeta = -\partial_x u - u_0 \partial_x \zeta. \end{aligned} \tag{14}$$

The new terms can be calculated with a centered in time scheme (calculated at time step n), but in that case, $\bar{w} = 0$ leads to unstable schemes when $u_0 \neq 0$. This probably explains the fact that the pure Euler forward–backward scheme is not possible in MICOM/HYCOM when advection is taken into account. However, at least when u_0 is not too strong there exist a threshold value for $\bar{w}$ over which the stability properties of the MICOM/HYCOM schemes without advection is recovered. This method has been

chosen by many other primitive equation codes (see for instance Ezer et al., 2002, and references therein) but would obviously lead to deep changes in the MICOM/HYCOM code.

Another alternative scheme is to keep the original MICOM/HYCOM schemes, except we now start integration of the fast barotropic equations at baroclinic time $(N-1)\Delta t_c$, instead of $N\Delta t_c$. This ensures stability for a pure advection, provided $\Delta t_c < \Delta x/u_0$, as it is now treated with the usual leapfrog scheme over the baroclinic time stepping (see Fig. 1). This is also easy to compute as it only requires modification of about 10 lines of the MICOM or HYCOM codes. However, this requires twice as many barotropic time steps as before, and thus doubles the cost of the barotropic scheme. This new scheme will be called LSBM: leapfrog for the slow part of the barotropic component.

4.2. Stability of alternative schemes

Fig. 4 is a comparison between the LSBM scheme (dashed line) and the original scheme (plain line) for $\bar{w} = 0.125,\ \Delta t_b = 0.75$ and different choices of $\Delta t_c = N_0 \Delta t_b$. For comparison, the dotted curve represents the CFL stability curve for a pure advective model with a leapfrog time stepping scheme. Notice that even though the stability properties of the LSBM scheme are still below the pure advective model characteristics (dotted curve) it is much better than the original MICOM/HYCOM one. In particular for a given advection u_0, the maximum baroclinic time step permitted is much larger (about twice the original value).

Fig. 5 is the same as Fig. 4; it represents a comparison between the LSBM scheme (plain line) and the original scheme (dashed line) for $\bar{w} = 0.75,\ \Delta t_b = 0.05$. Other choices for $\bar{w}$ lead to the same results, $\bar{w} = 0.75$ has only been chosen as it corresponds to the optimal choice for stability for the chosen time step for the original scheme (and the new one too). Notice that such small non-dimensional time steps are likely to be attained in shallow areas when a regional model extends over region with shallow and deep waters. Again, the results are the same as for Fig. 4: the LSBM is more stable than the original scheme but for small baroclinic time steps, it is now possible to reach much higher u_0, for larger baroclinic time steps, the two schemes become closer, even though the new one still has a better stability.

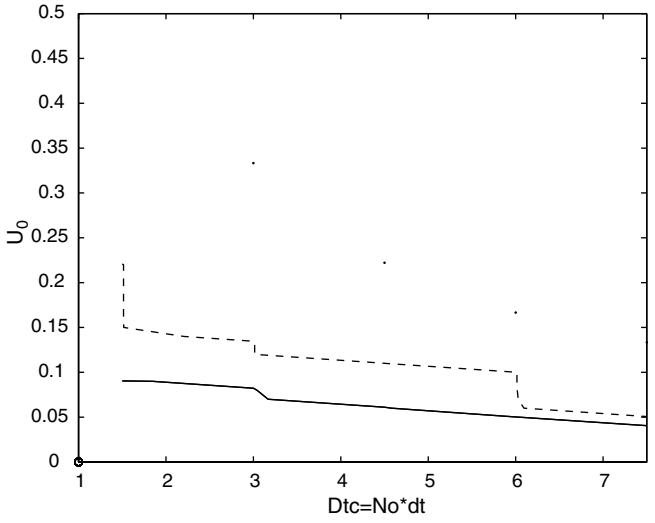

Fig. 4. Stability of the original MICOM/HYCOM scheme (plain line) compared to the stability of the LSBM scheme (dashed line) for $\Delta t_b = 0.75$ and $\bar{w} = 0.125$. Notice that the new scheme is always more stable. The dots represent the CFL criterion for a pure advection treated with a leapfrog scheme.

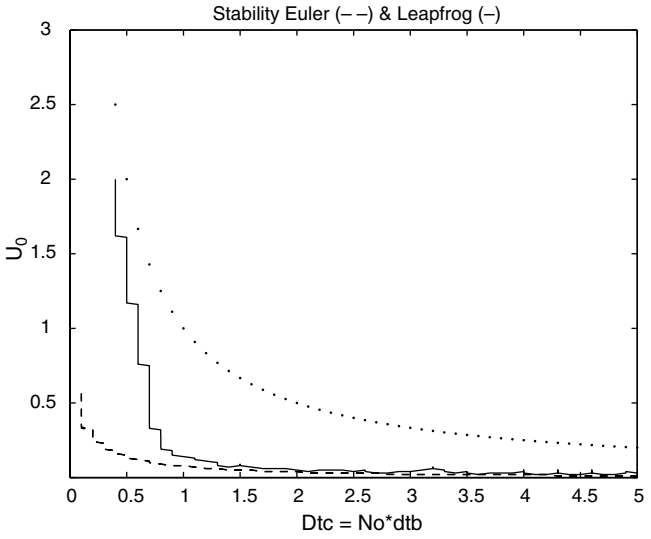

Fig. 5. Stability of the original MICOM/HYCOM scheme (plain line) compared to the stability of the LSBM scheme (dashed line) for $\Delta t_b = 0.05$ and $\bar{w} = 0.125$. Notice that the new scheme is always more stable. The dots represent the CFL criterion for a pure advection treated with a leapfrog scheme.

4.3. Application to realistic configurations

To deal with very shallow coastal waters, the advection term in the continuity equation has to be reintegrated as it becomes non-negligible and is thus important for the propagation of tidal gravity waves in regions were the current is strong (this term is then also important to properly calculate the mean currents over a tidal cycle). The previous stability calculations have been repeated with the full Eq. (2) instead of (5). The previous results and our conclusions are still valid: a leapfrog scheme for the slow part of the barotropic component leads to better stability properties.

In realistic configurations, where a basin or an oceanic region is modelled using a realistic bottom topography, and realistic forcing fields, the parameter u_0 varies spatially, because of the variable total depth of the ocean, and with time. It is thus interesting to evaluate its range of variation for different cases.

For basin scale models, the typical ocean depth varies from $H_0 \simeq 1000$ m or more to $H_0 \simeq 100$ m, and oceanic currents are rather weak at large scale, $U_0 \leqslant 0.1\ \mathrm{m\ s^{-1}}$ or so, but can reach $U_0 \simeq 1\ \mathrm{m\ s^{-1}}$ for strong oceanic currents. This yields a non-dimensional parameter $u_0 \in [0, 0.001]$ in the interior of the basin where large scale currents dominate and $u_0 \in [0, 0.03]$ near strong currents provided they are intensified in shallow regions (which is usually the case, as strong currents are often located along coastlines). Internal gravity waves then also provide a CFL condition that is in general more constraining than the CFL associated with advection that we have just discussed: the maximum propagation speed of internal gravity waves is indeed much higher than the maximum velocity. In such a context, the LSBM scheme is not expected to be necessary to ensure stability in general. Its use would therefore involve an increase of computational time that is not justified for such configurations.

When a regional model is developed and covers coastal areas, the typical ocean depth can vary from $H_0 \simeq 100$ m to $H_0 \simeq 1$ m, and oceanic currents can be pretty strong in coastal regions, for instance, tidal currents near Brittany, in France, can reach up to $U_0 \simeq 3$–$4\ \mathrm{m\ s^{-1}}$ in some shallow areas. This yields a maximum non-dimensional parameter $u_0 \simeq 2$, or even higher if shallower region are taken into account, which is the case when wetting and

drying regions are taken into account for instance. For such high values of u_0 the original MICOM/HYCOM scheme should have problems being stable, and the use of the new scheme presented here is necessary, the LSBM scheme being the easiest to compute, if not optimal for stability. In such configurations, the internal gravity waves also have small propagation speeds, and the overall CFL for the slow component is in general constrained by advection terms. The LSBM scheme should then improve the stability of the configuration and allow higher baroclinic time steps.

To illustrate this idea, we now discuss results from a high resolution barotropic configuration in the Golfe Normand Breton area (North-West of France). The HYCOM model has been used to model the tide dynamics in the area. Only one homogeneous layer is taken into account with a realistic bottom topography (see Fig. 6), the Mercator grid we use has grid steps varying from $\Delta X = 140$ m to $\Delta X = 150$ m, and the dynamics only takes into account the tide which is forced at the boundary using M2 and S2 modes from the MOG2D tide model (see Carrère and Lyard, 2003). The current can reach about 4 m s^{-1} for very intense tides. The model is started from rest on the 20th of September 1997 at 0h00 corresponding to a time period when very strong tides were generated. The model is run with the original HYCOM scheme and different choices of the baroclinic and barotropic time steps, and using the original schemes or the LSBM scheme. Notice that, to pursue the integration and avoid a model crash with the original scheme, we have imposed a limit to the total velocity: $U_{\max} = 5$ m s^{-1}.

Fig. 7 shows that noise develops in all configurations except the LSBM scheme (see Fig. 7d and f), which is the scheme that also allows the largest baroclinic time step. Also notice that reducing the barotropic time step from $\Delta t_b = 1.5$ s to $\Delta t_b = 0.5$ s in the original scheme leads to higher instability (compare Fig. 7a and b and notice the extended area of instability when Δt_b is decreased) a feature of the instability we have already discussed. Also notice that, as expected from the previous results, reducing the baroclinic time step from $\Delta t_c = 12$ s to $\Delta t_c = 6$ s for the original scheme improves stability, and can eradicate the numerical noise: Fig. 7c shows the results after 8h00 of integration in the region of strong velocity and the noise has indeed disappeared. Fig. 7d shows the results with $\Delta t_c = 12$ s but with the LSBM scheme. No noise is apparent here. Finally notice that $\Delta t_c = 6$ s is the minimum baroclinic time step that can be used with the original scheme (after 20h00 of integration, a zoom in Fig. 7e reveals some noisy contours in comparison with Fig. 7f).

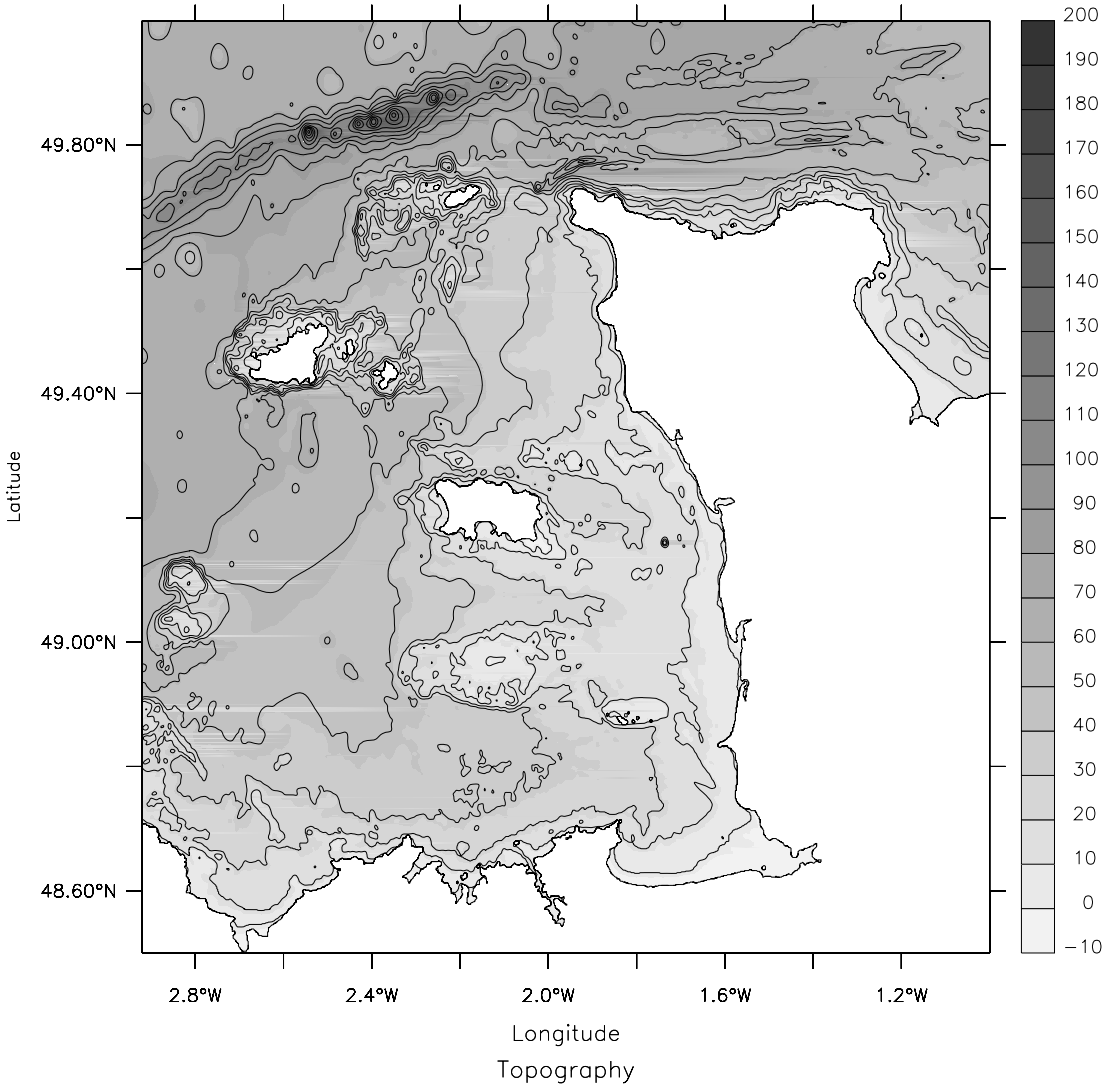

Fig. 6. Topography of the "Golfe Normand Breton" area.

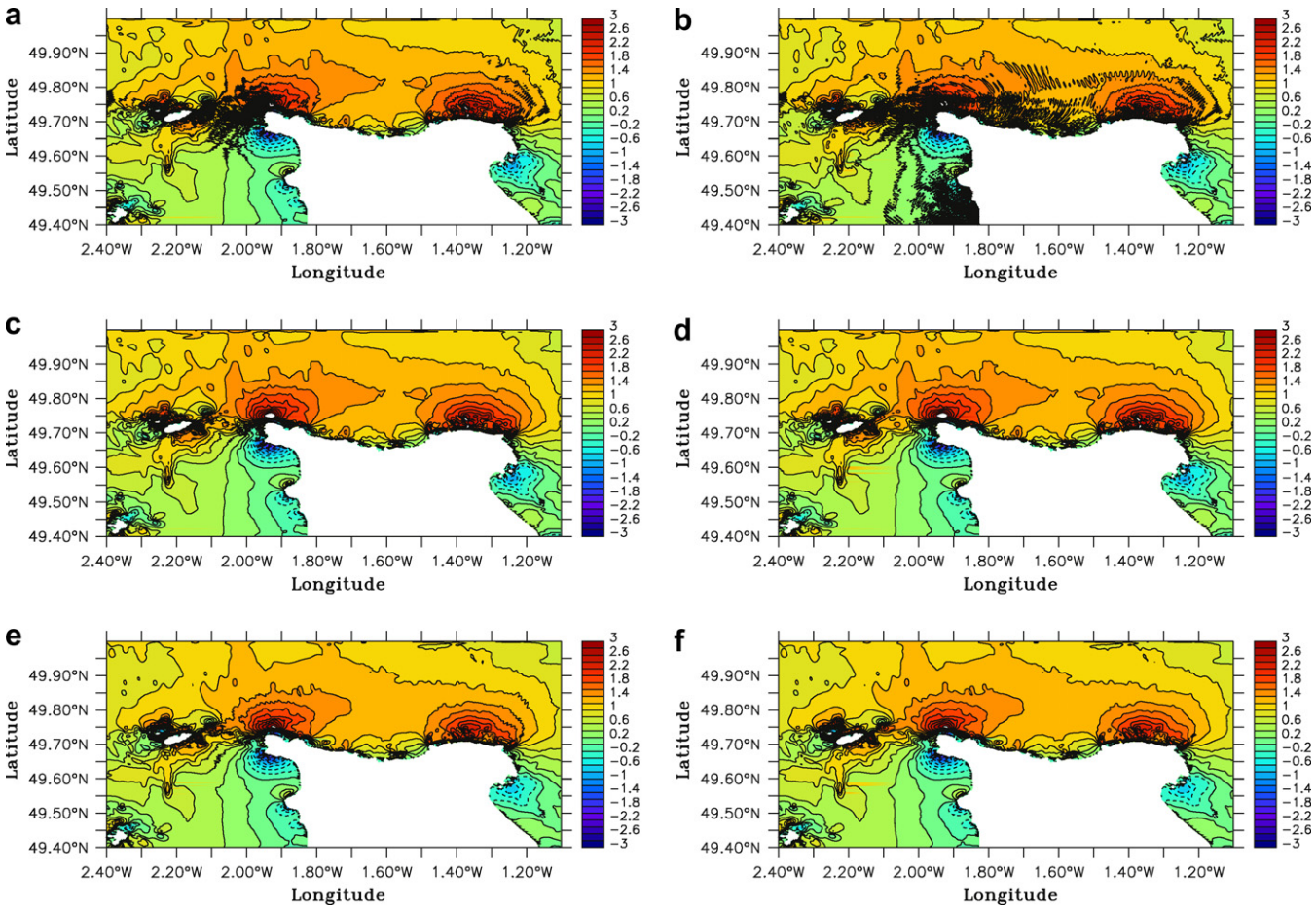

Fig. 7. Zoom of the Golfe Normand Breton configuration. Zonal velocity (in m/s) after 8h00 (a–d) or 20h00 (e, f) of integration of the HYCOM model and with different schemes and choices of parameters: original scheme with $\Delta t_c = 12$ s,$\Delta t_b = 1.5$ s (a); $\Delta t_c = 12$ s, $\Delta t_b = 0.5$ s (b); $\Delta t_c = 6$ s, $\Delta t_b = 1.5$ s (c,e). LSBM scheme with $\Delta t_c = 12$ s, $\Delta t_b = 1.5$ s (d,f). Notice that only the LSBM scheme remains stable.

5. Discussion

In the present paper, we have developed a method to analyse the linear stability of slow terms when integrated into the barotropic equations using time splitting techniques. Even though we have concentrated on the barotropic momentum advection, the method in Appendix B can be used for other terms too and can be useful for oceanic general circulation models in general, when they use time splitting.

We have then analysed and explained some instabilities we have experienced when using the HYCOM code to model shallow areas at high resolution. The barotropic advection term is indeed calculated with a centered spatial scheme but a Euler time stepping when averaged over the (baroclinic) slow time step of the model, which is unconditionally unstable. The instability can however be hidden when other terms are taken into account. The original scheme is indeed stabilised when adding the fast propagating barotropic gravity wave terms, given proper choices of the parameters Δt_b, Δt_c, $\bar{w}$. However, the stability is pretty reduced and Δt_c is strongly constrained by advection, in particular when the velocity becomes non-negligible in comparison with the gravity wave propagation speed, which is the case in shallow areas.

We have then proposed a simple way to improve this with a schemes (called LSBM) that only requires modest changes in the HYCOM code. The LSBM scheme doubles the computing time required for the barotropic component. However, as it allows the use of higher baroclinic time steps, there must exist a number of layers above which the LSBM scheme is more efficient than the original code (it requires less overall computing time to achieve a simulation). For instance, in the baie du Mont Saint–Michel configuration presented above, the cost of the original and LSBM schemes were nearly the same (given the fact that with the LSBM scheme, the baroclinic time step could be doubled), and there was only one layer. An extra layer would have doubled the additional cost of the original scheme in comparison with the LSBM scheme (again because of a reduced baroclinic time step), so that for such a configuration the LSBM scheme is more efficient as soon as two or more layers are taken into account. We have no clue however to prove it is the optimal scheme. For instance, including the advection term in the barotropic equation, is probably more efficient in some circumstances.

The cost of the configuration is a function of the number of horizontal grid points, the number of layers, the number of operations of the baroclinic and barotropic schemes, and the barotropic and baroclinic time steps. The LSBM scheme doubles the cost of the barotropic integration, but we have seen that it can induce a doubling of the baroclinic time step in comparison with the original scheme. We thus expect that it can be cost efficient (it can solve the same problem as the original scheme using less computational time) in some configurations, especially when the baroclinic time step is limited by the advection speed and with a configuration with many vertical layers. It is, however, difficult to define precisely when the LSBM scheme is optimal as it drastically depends on details of the configuration (depths range, maximum u_0

attained, stratification characteristics for the CFL associated with the maximum internal wave speed, ...). It is also worth mentioning that we have only addressed the optimality through an analysis of the stability properties, which is not completely objective. Indeed, the analysis should rather be based on the precision of the scheme (see Sanderson, 1998; Winther et al., 2007): the optimal scheme is the scheme that gives the result within a given precision for the smallest computational time. This is of course a much more complicated issue that is worth addressing, and the present work is only a first step toward this.

Finally, we have also proposed a new scheme for the fast barotropic equations (Eq. (18) in Appendix A). This new scheme could be of interest at least when the choice is made to incorporate the advection term in the fast barotropic equations, which is the case for many ocean models. This scheme indeed allows a far better stability (and probably a better precision as it allows larger $\bar{w}$ for the same time step) than the original scheme. For the HYCOM choice, with advection treated as a slow component, preliminary tests have revealed a strong dependency on N_0 (the number of barotropic time steps per baroclinic time steps) and $\bar{w}$, and more work is needed to address its effect on the stability of the slow part of the barotropic component.

Acknowledgements

The authors are supported by the French ministry of Defence and this work is part of the research program MOUTON (PEA 012401 funded by DGA and the French Navy) conducted by SHOM, the French Navy Hydrographic and Oceanographic Institute.

Appendix A. Numerical schemes for the fast barotropic mode

To focus on the numerical schemes for the fast barotropic mode, we can assume $u^* = 0$ in Eq. (10). To test for linear stability, we look for free solutions of the discretised equation (11) in the form

$$u_j^n = \hat{u}\lambda^n e^{ikj\Delta x},$$
$$\zeta_j^n = \hat{\zeta}\lambda^n e^{ikj\Delta x}. \tag{15}$$

For Eq. (11), λ then verifies

$$(\lambda^2 - (1-\bar{w})\lambda - \bar{w})^2 = -2(1+\bar{w})^2\Delta t^2(1-cos\theta)\lambda^3, \tag{16}$$

where $\theta = k\Delta x = k$.

The stability diagram of the HYCOM scheme is given by the plain line in Fig. 8, as a function of Δt and $\bar{w}$. In practice, the choice proposed in HYCOM is $\bar{w} = 0.125$, for which the maximum time step to ensure linear stability is $\Delta t \simeq 0.77$. Also notice that stability is impossible when $\bar{w}$ is close to 1. This is due to the fact that HYCOM mixes the time derivatives of both the leapfrog and Euler forward–backward schemes but only retains the spatial derivatives of the Euler forward–backward scheme. Other choices are possible. For instance, a more natural choice would be to mix the spatial derivatives of both schemes with the same weights as the time derivatives which would write

$$\zeta_j^{n+1} = (1-\bar{w})\zeta_j^n + \bar{w}\zeta_j^{n-1} - (1+\bar{w})\frac{\Delta t}{\Delta x}(u_{j+1}^n - u_j^n),$$
$$u_j^{n+1} = (1-\bar{w})u_j^n + \bar{w}u_j^{n-1} - (1-\bar{w})\frac{\Delta t}{\Delta x}(\zeta_j^{n+1} - \zeta_{j-1}^{n+1}) - 2\bar{w}\frac{\Delta t}{\Delta x}(\zeta_j^n - \zeta_{j-1}^n). \tag{17}$$

We have found that this would not yield satisfactory results in terms of stability. The dashed line in Fig. 8 indeed shows that with the latter choice, stability is recovered when $\bar{w}$ is close to 1, as we now recover the leapfrog scheme. However, the region of stability is almost everywhere drastically reduced, especially for small to moderate $\bar{w}$, which should allow the largest time steps.

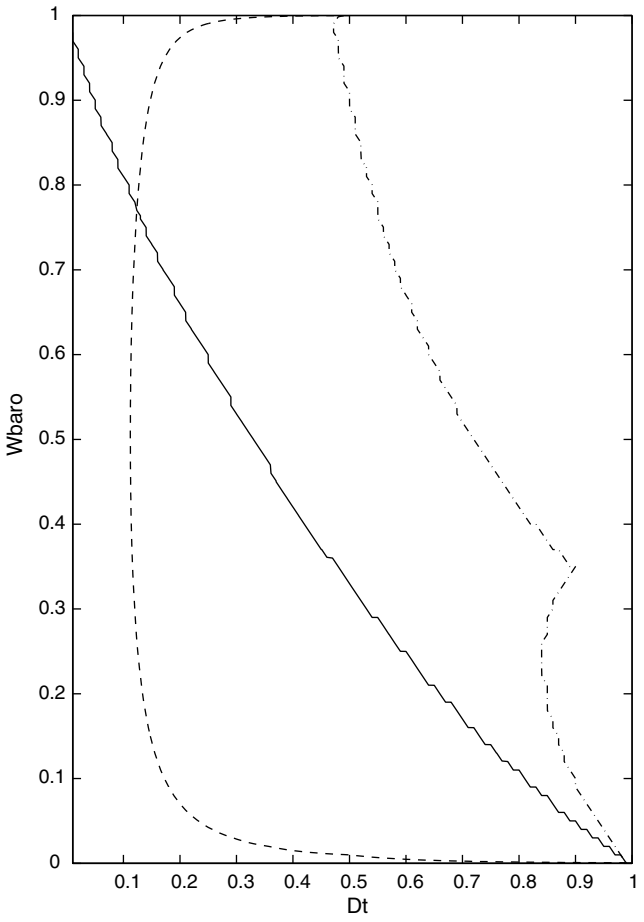

Fig. 8. Stability regions as a function of Δt and $\bar{w}$ for different barotropic schemes: the original MICOM/HYCOM code (plain line), the scheme proposed in Eq. (17) (dashed line) and the scheme proposed in Eq. (18) (dash–dotted line).

We have found that a better choice for the weights of the spatial terms is

$$\zeta_j^{n+1} = (1-\bar{w})\zeta_j^n + \bar{w}\zeta_j^{n-1} - (1+\bar{w})\frac{\Delta t}{\Delta x}(u_{j+1}^n - u_j^n),$$
$$u_j^{n+1} = (1-\bar{w})u_j^n + \bar{w}u_j^{n-1} - (1-\bar{w}^\alpha)\frac{\Delta t}{\Delta x}(\zeta_j^{n+1} - \zeta_{j-1}^{n+1}) - 2\bar{w}^\alpha\frac{\Delta t}{\Delta x}(\zeta_j^n - \zeta_{j-1}^n). \tag{18}$$

We have indeed found that the stability region was drastically expanded when $\alpha \simeq 1.5$. It is, in particular, always more stable than the choice made by HYCOM (see dash–dotted line in Fig. 8).

Finally, notice that the new scheme proposed here does not require a new implementation of other terms that were not considered here (the Coriolis terms for instance): the modifications only apply to the pressure gradient terms, and all other terms keep their original implementation.

Appendix B. Algorithm for the calculation of the stability of the slow component

To analyse the stability property of the model for the slow component, we proceed as follows.

First step

We consider the discretised version of the linearised equations (8)–(10) and rewrite them for perturbations of the form:

$$u_j^N = \hat{u}^N e^{ikj\Delta x},$$
$$\zeta_j^N = \hat{\zeta}^N e^{ikj\Delta x}. \quad (19)$$

This yields for the basic numerical schemes used in the HYCOM model:

$$u_j^{*,N} = -u_0(u_{j+1}^N - u_{j-1}^N),$$
$$= -u_0\hat{u}^N 2i\sin(k\Delta x)e^{ikj\Delta x}, \quad (20)$$

or

$$u^{*,N} = -u_0\hat{u}^N 2i\sin(k\Delta x), \quad (21)$$

and, for the fast mode integration (using only the pure Euler forward–backward scheme for simplification) from time step N – or $N-1$ for the LSBM scheme – (both corresponding to the fast index $n=0$) to $N+1$ (corresponding to the fast index $n = N_0 = \Delta t_c/\Delta t_b$ for the original MICOM/HYCOM scheme and $n = 2N_0$ for the LSBM scheme):

$$\hat{\zeta}^{n+1} = \hat{\zeta}^n - \Delta t_b\hat{u}^n(e^{ik\Delta x} - 1),$$
$$\hat{u}^{n+1} = \hat{u}^n - \Delta t_b\hat{\zeta}^{n+1}(1 - e^{-ik\Delta x}) + \Delta t_b u^* \quad (22)$$

Second step

As Eqs. (22) are linear, the components of the 2×2 matrices $\mathbf{A}_k$ and $\mathbf{B}_k$ (Eq. (13)) are constant and do not depend on $\hat{\zeta}$ or $\hat{u}$. We thus use particular combinations of $\hat{\zeta}^{N/N-1}$ and $\hat{u}^{N/N-1}$ (corresponding the initial barotropic step $n=0$ and the constant forcing associated with u^*) to calculate them numerically from the iteration of Eq. (22).

$$(\hat{\zeta}^{N/N-1}, \hat{u}^{N/N-1}) = (0,1),(1,0),(0,0). \quad (23)$$

For the original HYCOM scheme, as $n=0$ corresponds to baroclinic time step N, $\hat{\zeta}^{N-1}$ and $\hat{u}^{N-1}$ do not intervene and $\mathbf{B}_k$ is null. This is not the case for the LSBM scheme.

Final step

Once the coefficients of the matrices are known, the linear stability of the numerical system for the wavenumber k is given by the solutions of the equation (again, we seek solutions of the form $\hat{\zeta}^N = \hat{\zeta}\lambda^N$):

$$\mathrm{DET}(\lambda^2\mathrm{Id} - \lambda A_k - B_k) = 0, \quad (24)$$

where DET is the determinant of the 2×2 matrix and Id is the identity matrix. The analysis is performed for wavenumber $k \in [0,\pi]$ to evaluate the overall stability for given parameters of the numerical schemes.

The same is done for general HYCOM schemes including $\bar{w}$ in Eq. (22) or for alternative schemes.

Remark

Notice that the previous analysis is only possible if the initial fast time step only takes into account the fields at $n=0$. Indeed, if for instance the leapfrog scheme is used initially taking into account the fast time step $n=-1$ (corresponding to the step before the last of the previous barotropic iteration), then the fields at the slow time step N has to be expressed as a function of ALL previous slow time steps $(0,1,\ldots,N-1)$ and the stability analysis is in principle impossible. This is the case of the original MICOM or HYCOM scheme, but in practice, when the number of fast iterations is large the initial iteration is forgotten and the stability of the overall scheme should not be very different from the same scheme with a first step using a full Euler forward–backward step.

References

Arakawa, A., Lamb, V., 1977. Computational design of the basic dynamical processes of the ucla general circulation model. Methods Comput. Phys. 17, 174–267.

Bleck, R., 2002. An oceanic general circulation model framed in hybrid isopycnic-cartesian coordinates. Ocean Modell. 4, 55–88.

Bleck, R., Boudra, B., 1986. Wind-driven spin-up eddy-resolving ocean models formulated in isopycnic and isobaric coordinates. J. Geophys. Res., 7611–7621.

Bleck, R., Rooth, C., Hu, D., Smith, L., 1992. Salinity driven thermocline transients in a wind and thermohaline forced isopycnic coordinate model of the North Atlantic. J. Phys. Oceanogr. 22, 1486–1505.

Bleck, R., Smith, L., 1990. A wind-driven isopycnic coordinate model of the north and equatorial Atlantic Ocean 1. Model development and supporting experiments. J. Geophys. Res. 95 (C6), 3273–3285.

Carrère, L., Lyard, F., 2003. Modeling the barotropic response of the global ocean to atmospheric wind and pressure forcing – comparisons with observations. Geophys. Res. Lett. 30, 1–8.

Cushman-Roisin, B., 1994. Introduction to Geophysical Fluid Dynamics. Prentice-Hall Inc. 320pp.

Ezer, T., Arango, H., Shchepetkin, A., 2002. Developments in terrain-following ocean models: intercomparisons of numerical aspects. Ocean Modell. 4, 249–267.

Hallberg, R., 1997. Stable split time stepping schemes for large-scale ocean modeling. J. Comp. Phys. 135, 54–65.

Higdon, R., Bennet, A., 1996. Stability analysis of operator splitting for large-scale ocean modeling. J. Comp. Phys. 123, 311–329.

Pedlosky, J., 1987. Geophysical Fluid Dynamics. Springer, New York. p. 710.

Sanderson, B.G., 1998. Order and resolution for computational ocean dynamics. J. Phys. Oceanogr. 28, 1271–1286.

Shchepetkin, A., McWilliams, J., 2005. The regional oceanic modeling system (roms): a split-explicit, free-surface, topography-following-coordinate oceanic model. Ocean Modell. 9, 347–404.

Winther, N., Morel, Y., Evensen, G., 2007. Efficiency of high order numerical schemes for momentum advection. J. Mar. Sys. 67, 31–46.